

Ion beam microanalysis of human hair follicles

Zs. Kertész^{a,*}, Z. Szikszai^a, P. Pelicon^b, J. Simčič^b, A. Telek^c, T. Bíró^c

^a Institute of Nuclear Research of the Hungarian Academy of Sciences, H-4001 Debrecen, P.O. Box 51, Hungary

^b Jožef Stefan Institute, Jamova 39, P.O. Box 3000, Ljubljana, Slovenia

^c Department of Physiology and Cell Physiology Research Group of the Hungarian Academy of Sciences, University of Debrecen, Medical and Health Science Center, Research Center for Molecular Medicine, H-4012, Debrecen, Nagyerdei krt. 98, Hungary

Available online 14 February 2007

Abstract

Hair follicle is an appendage organ of the skin which is of importance to the survival of mammals and still maintains significance for the human race – not just biologically, but also through cosmetic and commercial considerations. However data on composition of hair follicles are scarce and mostly limited to the hair shaft.

In this study we provide detailed information on the elemental distribution in human hair follicles in different growth phases (anagen and catagen) using a scanning proton microprobe.

The analysis of skin samples obtained from human adults undergoing plastic surgery and of organ-cultured human hair follicles may yield a new insight into the function, development and cyclic activity of the hair follicle.

© 2007 Elsevier B.V. All rights reserved.

PACS: 87.58.–b; 87.64.Gb; 87.64.Ee; 82.80.Ej; 82.80.Yc; 87.59.Jq

Keywords: Hair follicle; Growth phase; Elemental distribution; Microanalysis; Micro-PIXE; Scanning proton microprobe

1. Introduction

In mammals, hair follicles produce hair which has a diverse range of functions; it participates in thermoregulation, protects against trauma, collects sensory information, indicates sexual development and may aid in camouflage for survival. The total number of hair follicles for an adult human is estimated at 5 million and the only external regions of skin devoid of hair follicles are the palms and soles of the feet.

Recently the elemental composition of the epidermal layer of human skin has gained much attention due to, among others, the NANODERM project which investigates the penetration of micronized TiO₂ particles into

the skin [1–3]. However, data on skin appendages (such as the hair follicle which is a central mini-organ of the tissue with marked regeneration power) are scarce and mostly limited to the investigation of the hair shaft itself [4,5]. In addition, to the best of our knowledge, no data are available concerning the distribution of elements in human hair follicle with various growth and cycling phases.

In this study we provide detailed quantitative elemental distribution of organ-cultured hair follicle in anagen and catagen growth phases using ion microscopy in order to reach a better understanding of the function, development and cyclic activity of the hair follicle. The microprobe analysis was carried out at the scanning ion microprobe facilities at the Institute of Nuclear Research of the Hungarian Academy of Sciences, Debrecen, Hungary [6–8] and at the Jožef Stefan Institute, Ljubljana, Slovenia [9], using combined STIM and PIXE ion beam analytical techniques.

* Corresponding author. Tel.: +36 52 509200; fax: +36 52 416181.
E-mail address: zsofi@atomki.hu (Zs. Kertész).

2. Hair follicle morphology and growth cycle

2.1. Structure of hair follicles

Fig. 1 shows hematoxylin–eosin stained sections of hair follicles (HF) in different growth phases. The structure of the HF can be well followed on the “anagen” HF.

Hair follicle can be recognised as a separate entity within the skin with formation and maintenance based on interaction between dermal and epidermal components. At the heart of the hair follicle lies the *dermal papilla* (DP). The dermal papilla consists of a highly active group of cells shown to be capable of inducing follicle development from the epidermis and production of hair fibre. The dermal papilla is covered and surrounded by *matrix keratinocyte cells*. These are living, actively proliferating group of cells which differentiate and become keratinized to form the *hair shaft* (HS).

The hair shaft is surrounded by two sheaths – the *inner root sheath* (IRS) and *outer root sheath* (ORS). These sheaths protect and mould the growing hair shaft. The inner sheath follows the hair shaft and ends below the opening of a sebaceous gland. The outer sheath continues all the way up to the gland. A sebaceous (‘oil’) gland opens into each hair follicle and produces sebum, a lubricant for the hair and skin that helps repel water, damaging chemicals and micro-organ-

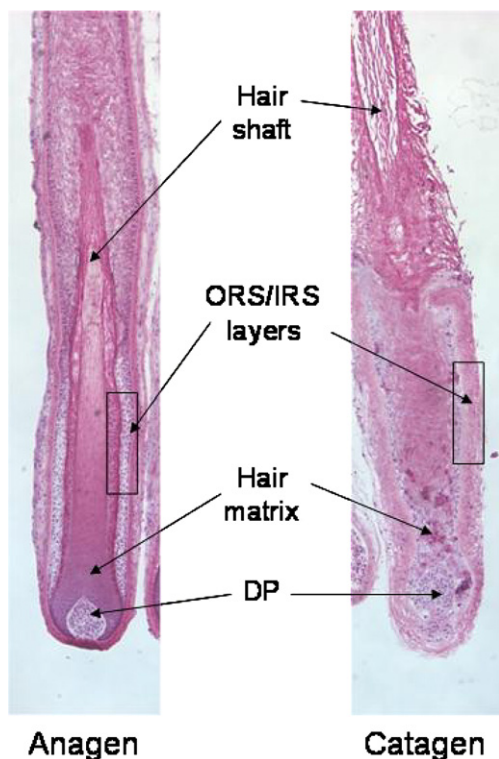


Fig. 1. Morphology of anagen and catagen HFs. Organ-cultured anagen HFs were treated with either vehicle (Anagen) or 10 μ M capsaicin (Catagen) for 5 days and then processed for HE-staining routine histology. Caption: DP, dermal papilla; ORS, outer root sheath; IRS, inner root sheath. Original magnification, 40 \times .

isms. Small *arrector pili* muscle fibres are attached to each hair follicle.

2.2. Hair follicle cycle

Under normal circumstances hair growth in each follicle occurs in cycles. There are three main phases of the hair growth cycle: anagen, catagen and telogen (see Fig. 1). *Anagen* is the active growth phase when hair fibre is produced. This stage lasts about 2–6 years. This is followed by the *catagen phase*, a period of controlled regression of the follicle, which lasts 1–2 weeks and during which the dermal papilla condenses as the cells become inactive and the hair follicle shrinks to about 1/6 of the normal length. Finally the hair follicle enters the *telogen phase*, the resting state. This lasts about 5–6 weeks, the dermal papilla becomes isolated and the hair fibre can be easily pulled out.

3. Sample description

3.1. Isolation and maintenance of hair follicles

Human anagen hair follicles were isolated from skin obtained from females undergoing face-lift surgery [10]. Isolated HFs were maintained in 24-multiwell plates in Williams E medium (Biochrom, Cambridge, UK) supplemented with 2 mM L-glutamine (Invitrogen, Paisley, UK), 10 ng/ml hydrocortisone (Sigma–Aldrich, Taufkirchen, Germany), 10 μ g/ml insulin (Sigma) and antibiotics.

3.2. Induction of catagen transformation

As we have previously shown, the activation of the vanilloid receptor-1 (TRPV1) – expressed mostly in the epithelial layers of organ-cultured HFs such as the outer root sheath (ORS) and matrix keratinocytes – by the agonist capsaicin resulted in the inhibition of proliferation, induction of apoptosis and the initiation of catagen transformation [11]. Therefore, cultured anagen HFs were treated by either vehicle or by 10 μ M capsaicin for 5 days.

3.3. Sample processing

Cultured HFs were then embedded to Killik cryostat embedding medium (Bio-Optica, Milan, Italy) and cryostat sections of various thickness (5–25 μ m) were prepared. For determination of morphology, a routine histology was performed using hematoxylin–eosin (HE) staining (Sigma).

For microprobe analysis 20 μ m thick cryostat sections were mounted on thin pioloform foil. The sections were freeze-dried in the atmosphere of the cryostat under -25°C .

4. Microprobe analysis

Microprobe analysis of the samples was carried out at the Debrecen Scanning Ion Microprobe and at the Ljublj-

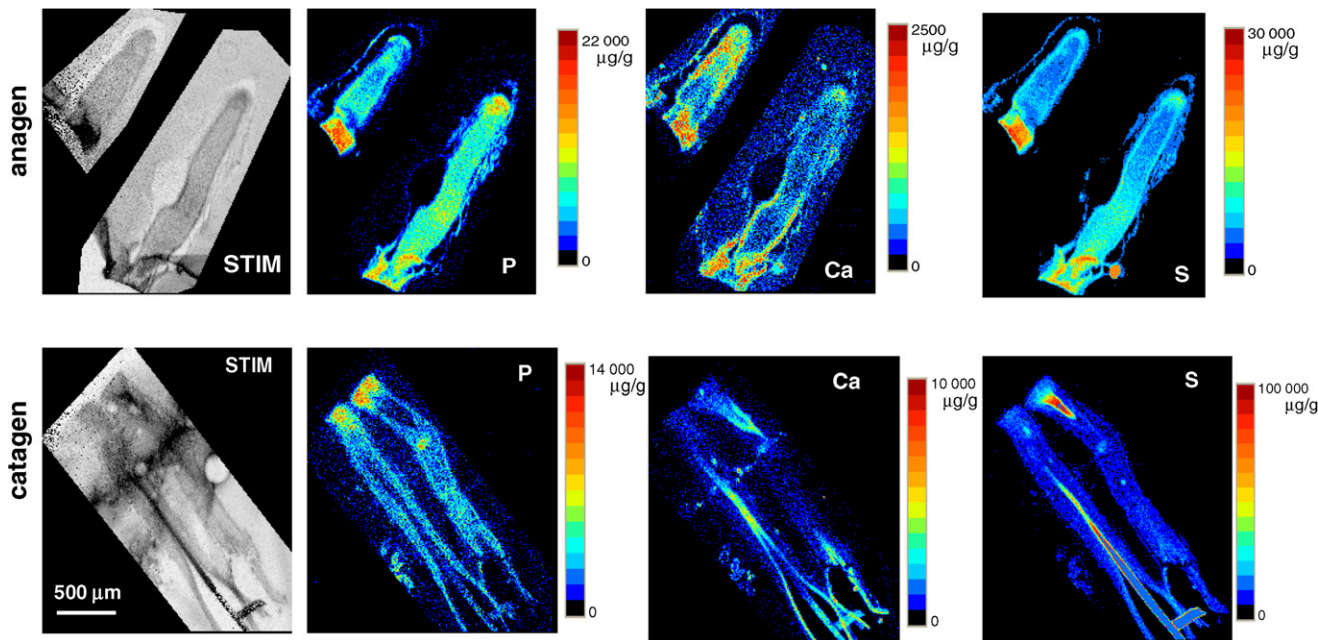


Fig. 2. Median energy STIM map and P, S and Ca true elemental maps of anagen and catagen hair follicle.

ana Ion Microprobe. Combined on-axis STIM and PIXE ion beam analytical techniques were used to analyse the samples. STIM spectra and maps were used to determine the morphology and the area density of the samples. PIXE spectra and maps obtained with Si(Li) and HP Ge X-ray detectors were used to quantify the concentrations and distributions of elements heavier than Na. The accumulated charge irradiating the sample was measured with a beam chopper. More detailed description of the measurement setup can be found in [12,13].

A 2 MeV proton beam of 100–300 pA current focused to $2 \times 2 \mu\text{m}^2$ was used to irradiate the samples. The total accumulated charge collected during each measurement varied between 0.8 and 1.5 μC .

In order to determine the mass loss due to the irradiation and the extent of the shrinkage, on-axis STIM maps were taken before and after the PIXE measurements. During the hair follicle measurements shrinkage of the samples was not observed. Due to the relative low currents used for the irradiation the mass loss of the samples remained under 5%.

True elemental maps and absolute concentration values were evaluated from the obtained STIM and PIXE list mode data with the PIXEKLM-TPI program package [14,15].

5. Results and discussion

Elemental distributions and absolute concentrations were determined along 5 capsaicin treated (catagen) and 4 control (anagen) hair follicles. The investigated length varied between 1.5 and 2 mm. Average elemental concentration values of the whole sample and the different mor-

phological parts were also determined. STIM energy maps and P, S and Ca true elemental maps of an anagen and a catagen HF are presented on Fig. 2.

The different parts of the HF can be well identified on the histological images (Fig. 1) as well as on the obtained elemental maps (Fig. 2). The ORS can be characterised by high concentration of phosphorous, since it corresponds to the stratum spinosum layer of the epidermis. The IRS, the counterpart of the stratum corneum, is characterised by high Cl and S concentrations. Very high concentration of S is characteristic to the hair shaft, while the matrix cells contains phosphorous in high concentration.

Concentrations for most of the elements were found to be the same in the corresponding parts of the anagen and the catagen hair follicles. However significant differences were observed in the Ca concentration between the anagen and catagen HFs.

With respect to the distribution of Ca, in anagen (control) HFs, the following concentrations were measured (given in $\mu\text{g/g}$ dry weight): DP, ~ 500 ; matrix of the bulb, 1000–1500; ORS/IRS keratinocyte layers, 1000–2000; hair shaft, 1000–2000. The induction of catagen transformation essentially did not change the Ca concentrations in the DP, bulb matrix regions nor in the hair shaft (1000–2000 in all parts). However, we observed a remarkable increase in the ORS/IRS keratinocyte layers up to 4000–8000 $\mu\text{g/g}$ Ca concentration.

6. Conclusion

In capsaicin-treated catagen HFs, the Ca concentration was increased mostly in those layers which possess a significant expression of TRPV1, the receptor for capsaicin [11].

Since TRPV1 functions as a Ca-permeable channel [16], the elevated Ca in the TRPV1-expressing layers suggest that the activation of TRPV1 by capsaicin resulted in a prolonged elevation of intracellular Ca-concentration which, in turn, led to the inhibition of proliferation of HF keratinocytes as well as the induction of HF apoptosis. Moreover, our findings also show that ion microscopy may serve as a fine tool to detect changes in elemental distribution related to the human hair-cycle.

Acknowledgement

This work was supported by the Hungarian-Slovenian Intergovernmental S&T Cooperation programme (Contract No. OMF0427/2006) and the Hungarian Research Foundation (OTKA) under contract no. K063153.

References

- [1] F. Menzel, T. Reinert, J. Vogt, T. Butz, Nucl. Instr. and Meth. B 219–220 (2004) 82.
- [2] Zs. Kertész, Z. Szikszai, E. Gontier, P. Moretto, J.-E. Surlève-Bazeille, B. Kiss, I. Juhász, J. Hunyadi, Á.Z. Kiss, Nucl. Instr. and Meth. B 231 (2005) 280.
- [3] J. Pallon, M. Garmer, V. Auzelyte, M. Elfman, P. Kristiansson, K. Malmqvist, C. Nilsson, A. Shariff, M. Wegdén, Nucl. Instr. and Meth. B 231 (2005) 274.
- [4] R.W. Ollerhead, G.J.F. Legge, Nucl. Instr. and Meth. B 40 (1989) 664.
- [5] Ph. Moretto, J.E. Surlève-Bazeille, D. Licu, C. Michelet, P. Stoedzel, Nucl. Instr. and Meth. B 158 (1999) 386.
- [6] Rajta, I. Borbély-Kiss, Gy. Móri, L. Bartha, E. Koltay, Á.Z. Kiss, Nucl. Instr. and Meth. B 109–110 (1996) 148.
- [7] Simon, G. Kalinka, Nucl. Instr. and Meth. B 231 (2005) 507.
- [8] G.Á. Sziki, I. Uzonyi, E. Dobos, I. Rajta, K.T. Biró, S. Nagy, Á. Kiss, Nucl. Instr. and Meth. B 219–220 (2004) 508.
- [9] J. Simčič, P. Pelicon, M. Budnar, Ž. Šmit, Nucl. Instr. and Meth. B 190 (2002) 283.
- [10] M.P. Philpott, M.R. Green, T. Kealey, J. Cell Sci. 97 (1990) 463.
- [11] E. Bodó, T. Bíró, A. Telek, G. Czifra, Z. Griger, I.B. Tóth, A. Mescalchin, T. Ito, A. Bettermann, L. Kovács, R. Paus, Am. J. Pathol. 166 (2005) 985.
- [12] Zs. Kertész, Z. Szikszai, I. Uzonyi, A. Simon, Á.Z. Kiss, Nucl. Instr. and Meth. B 231 (2005) 106.
- [13] P. Pelicon, J. Simčič, M. Jakšić, Z. Medunić, F. Naab, F.D. McDaniel, Nucl. Instr. and Meth. B 231 (2005) 53.
- [14] Gy. Szabó, I. Borbély-Kiss, Nucl. Instr. and Meth. B 75 (1993) 123.
- [15] Uzonyi, Gy. Szabó, Nucl. Instr. and Meth. B 231 (2005) 156.
- [16] M.J. Caterina, M.A. Schumacher, M. Tominaga, T.A. Rosen, J.D. Levine, D. Julius, Nature 389 (1997) 816.